Automated Nuclei Segmentation Approach based on Mathematical Morphology for Cancer Scoring in Breast Tissue Images

Aymen Mouelhi[1], Mounir Sayadi[1], Farhat Fnaiech[1], and Karima Mrad[2]
[1]Laboratory of Signal Image and Energy Mastery, ENSIT-University of Tunis, Tunisia.
[2]Morbid Anatomy Service, Salah Azaiez Institute of Oncology, Tunisia

Abstract: *In this work, we propose an automated approach able to perform accurate nuclear segmentation in immunohistochemical breast tissue images in order to provide quantitative evaluation of estrogen or progesterone receptor status that will help pathologists in their diagnosis. The presented method is based on color deconvolution and an enhanced morphological processing, which is used to identify positive stained nuclei and to separate all clustered nuclei in the microscopic image for a subsequent cancer scoring. Experiments on several breast cancer images of different patients admitted into the Tunisian Salah Azaiez cancer center, show the efficiency of the proposed method when compared to the manual evaluation of experts. On the whole image database, we recorded more than 97% for both accuracy of detected nuclei and cancer scoring over the truths provided by experienced pathologists.*

Keywords: *Breast cancer, immunohistochemical image analysis, color deconvolution, morphological operators.*

Received September 11, 2014; accepted March 23, 2015

1. Introduction

Manual assessment of Estrogen (ER) and Progesterone (PR) receptor status from Immunohistochemical (IHC) breast tissue images is a subjective, time consuming and error prone process [2, 4, 5, 11]. Automatic image analysis methods offer the possibility to get consistent, objective and rapid diagnoses of histopathology specimens. Recently, with the continuing developments in computer technology, high-throughput tissue slide scanners, these methods have gained more and more importance as they are able to give accurate quantitative measurements of antigen activations and uniform indicators of cancer evolution [2, 11]. In IHC images with nuclear activity, stained nuclei are classified into three categories according to their color and shape features, i.e., Positive cancer nuclei (P), Negative cancer nuclei (N) and Benign nuclei (B). Positive cancer nuclei are labeled by brown color while negative and benign nuclei are marked by blue color. Benign nuclei such as lymphocytes, stromal cells are identified with their small size and elliptic shape shown in Figure 1.

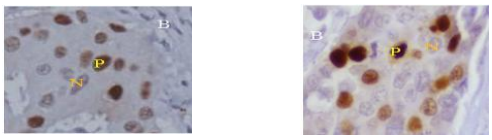

Figure 1. Example of stained breast tissue images with nuclear activity.

These non-cancerous nuclei are not needed in the cancer diagnosis process since the pathologist's medical treatment are based mainly on the ratio of the number of positive nuclei to the total number of cancer cell nuclei in the whole image [5, 11].

As illustrated in Figure 1, it's obvious that breast cancer tissue images presents many inherent characteristics such as staining inhomogeneity, stains superposition, uneven background, morphological variations of cancer nuclei, the presence of a multitude of touching nuclei and spurious cells, that can cause many difficulties to the classical nuclear segmentation methods. So, these challenging problems motivate researchers to design and develop ad-hoc approaches for the segmentation and the analysis of IHC tissue images.

In the last few years, many promising tissue segmentation methods are proposed in the literature which can reliably segment cancer cell nuclei and overcome the limitations of manual approach. Most of these methods contain two parts. The first one is generally related to the substance classification in the stained tissue (e.g., nuclei, cytoplasm, stroma, and background) which is done using of automatic multithresholding [9], supervised and/or unsupervised clustering based methods or color deconvolution techniques [1, 10, 12]. The second part deals with the separation of clustered and touching nuclei in the image. This problem can be solved by advanced morphological techniques such as improved watershed algorithms [3, 8] and ellipse fitting procedures.

In this work, we present a fully automated nuclear segmentation method based on stains separation using the color deconvolution technique combined with an improved morphological procedure for cancer nuclei segmentation and quantification. In fact, the combination of color separation techniques and morpholgical operators already exists in the literature and it's generally applied to solve the problem of nuclei quantification in IHC tissue images with cytoplasm or membrane activations [1, 2]. However, color and morphological features of cell nuclei is exploited in our work to segment breast tissue images with nuclear activity. Besides, clustered nuclei are splited here by our enhanced watershed algorithm based on a concave vertex graph, followed by an adaptive morphological procedure to remove benign nuclei and stromal cells from the segmented nuclei. In fact, many state-of-art methods are proposed in this field in order to give accurate segmentation results of cancer nuclei. The majority of these methods are based on marker-controlled watershed [3, 13] or region merging watershed [8] which are more sophisticated than traditional algorithms in term of splitting accuracy. However, shape information of cell nuclei is weakly included or completly ingnored in these algorithms which leads in some cases to over-segmented or under-segmented nuclei. In our work, we have integrated the shape information of clustered nuclei using high concavity points in the nuclei contours in order to ref ine the watershed results. This technique takes into consideration nuclear configurations and color gradient information within nuclei that garantee in most cases efficient segmentation results. In summury, the main contribution of the present work is the proposal of an automatic nuclear segmentation scheme which combines color deconvolution method and an improved morphological technique in order to study its ability in evaluating ER or PR status of breast cancer specimens.

The rest of the paper is organized as follows: in section 2, we present the segmentation method to detect and segment cancer nuclei in IHC stained tissue images. Experimental results of the proposed method are presented and discussed in section 3. Finally, section 4 contains a summary and conclusions.

2. The Proposed Method

As illustrated in Figure 2, the proposed nuclear segmentation method is composed mainly of two steps: Color separation and cancer nuclei segmentation. For the first step we applied a color deconvolution approach [12] in order to extract brown component and blue component from the RGB image. However, for cancer nuclei segmentation we developed custom-designed methods based on morphological techniques.

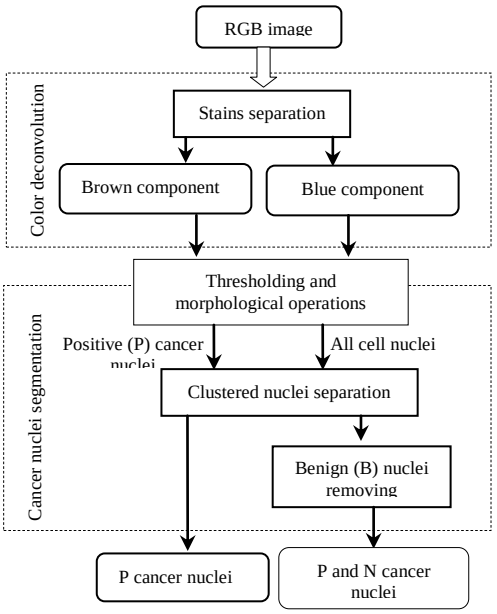

Figure 2. Flow chart of the proposed nuclear segmentation method.

In this step we start with an adaptive thresholding for each stain followed by morphological operations to detect properly stained nuclei in the tissue. From the brown component only positive cancer nuclei are selected whereas, by tresholding of the blue component we obtain all cell nuclei regions in the image. Then, clustered and touching nuclei are separated using an enhanced watershed method which takes into consideration the shape changes of nuclei and color gradient information within nuclei. This technique is applied on the two binary images corresponding to the positive cancer nuclei and all stained nuclei in the tissue. After that, to get the total number of cancer nuclei (i.e., positive and negative cancer nuclei), an adaptive morphological criterion is designed to remove benign nuclei and spurious cells from the segmented image of all nuclei. Finally, the percentage of positive staining can be easily computed by the ratio of the number of positive cancer nuclei to the total number of positive and negative nuclei in the whole image. Cancer score is identified subsequently using the clinical scoring protocol [7] shown in Table 1. Details of the proposed method are given below.

Table 1. The scoring system used for ER/PR positive status evaluation.

Score	Proportion of positive nuclear staining (%)
0	0 – 10
1+	11 – 33
2+	34 – 66
3+	67 – 100

2.1. Color Deconvolution

In the first step of the proposed nuclear segmentation method, we simply used the color deconvolution method developed by Ruifrok and Johnston [12] in order to separate brown (3, 3-Diaminobenzidine (DAB) staining) and blue (Hematoxylin (H) staining)

components of the RGB image. This technique is widely applied in the recent IHC image analysis approaches since it was shown to achieve better results than classical color segmentation methods in presence of stains' colocalization, which is a frequent phenomenon in IHC imaging due to the chemical reactions of stains and tissue superposition [2, 12]. With this method color information carried by the two stains can be de-convolved by determining the relative contributions of each of the RGB color channels to the specific stain. Color deconvolution parameters can vary according to the used dyes in histopathology and the imaging protocols [1]. So, to use this technique appropriately, we followed the suggestions given by Ruifrok and Johnston [12] and we determined the proper parameters for the protocols of our laboratory. First, the monochromatic pixel values (Red, Green, Blue) are converted to Optical Density (OD) values according to the equation below [12]:

$$OD_{R,G,B} = -log_{10}\left(\frac{I_{R,G,B}}{(I_{R,G,B})_{blank}}\right) \quad (1)$$

Where $OD_{R,G,B}$ are the optical density values for each colour component and $(I_{R,G,B})_{blank}$ are the pixel values for the image of the blank field. Then, parameters of color deconvolution are obtained for each stain by inversing the normalized *OD* matrix [12].

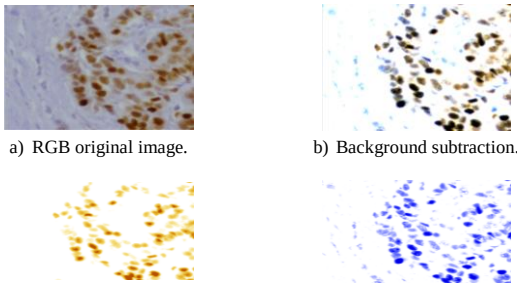

a) RGB original image. b) Background subtraction.

c) Colour deconvolution results detecting the contribution of H (blue) staining. d) Colour deconvolution results detecting the contribution of DAB (brown) staining.

Figure 3. Stains separation.

To achieve the best performance from color deconvolution, background subtraction with color correction is applied to the IHC images before processing. The contrast is first enhanced through intensity histogram equalization. Then, stained nuclei are highlighted by adding the resulting image to the intensity image adjusted by a linear contrast stretching shown in Figure 3-b. The new stain vectors are determined experimentally in our laboratory by the following equations:

$$DAB\ (brown) = (0.4475 \times R) + (0.5124 \times G) + (0.9837 \times B) \quad (2)$$

$$H\ (blue) = (0.9408 \times R) + (0.8124 \times G) + (0.3767 \times B) \quad (3)$$

In Figures 3-c and d we show respectively color deconvolution results separating the contributions of H (blue) and DAB (brown) staining to an original IHC image. The main steps of the color deconvolution method are summarized as follows:

- *Step 1*. Given the RGB microscopic image, enhance the image contrast through intensity histogram equalization.
- *Step 2*. Add the resulting image to the intensity image adjusted by a linear contrast stretching to highlight to stained nuclei.
- *Step 3*. Compute the stain vectors using the color deconvolution parameters given by (2) and (3).

2.2. Cancer Nuclei Segmentation

2.2.1. Adaptive Thresholding and Morphological Operations

As seen in Figure 3, the obtained nuclei regions from the color separation technique are characterized by intensity variations due to the noise and stain inhomogeneity. So, the possibility to find one threshold that can fit the entire image becomes a difficult task in our situation. This leads to the conclusion that an adaptive local throsholding will be more suitable than global thresholding because of its ability to minimize the effects of unrepresentative pixel values in the image [2]. In our work, an adaptive threshold is selected for each pixel based on the intensity distribution in its local neighborhood. This is done by subtracting each pixel's intensity by the median value of its neighborhood [2]. The neighborhood size is chosen here according to the average area of the nuclei which is mainly dependent on image amplification: We empirically set in our implementation a value of 22, 44 and 140 for IHC images acquired with a magnifying factor ×20, ×40 and ×80, respectively.

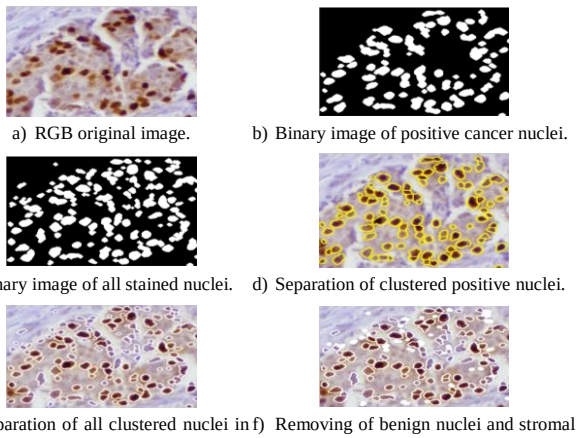

a) RGB original image. b) Binary image of positive cancer nuclei.

c) Binary image of all stained nuclei. d) Separation of clustered positive nuclei.

e) Separation of all clustered nuclei in the image. f) Removing of benign nuclei and stromal particles.

Figure 4. Main steps of cancer nuclei segmentation.

To overcome intensity variations inside nuclei and irregular nuclear configurations we applied some morphological operations to the two binary images. The transformed images of positive nuclei staining and all stained nuclei are represented respectively in

Figures 4-b and c. They are obtained after three successive procedures: Dilatation, opening and holes filling.

2.2.2. Clustered and Touching Nuclei Separation

In order to separate touching or overlapping nuclei, an enhanced watershed method is applied in this work to the detected nuclei regions for each binary image. In the proposed watershed method [11], shape information about clustered nuclei is exploited in a simple way to refine results of the classical watershed algorithm. In fact, to get initial separating curves of clustered cell nuclei, we have applied the watershed algorithm by immersion [14] on a gradient-weighted distance transform. The distance transform combines two image transformations: The geometric distance transform and the intensity gradients transform. It takes into consideration nuclear configurations and color gradient information within nuclei [8]:

$$D' = D \times exp\left(1 - \frac{\Lambda - \Lambda_{min}}{\Lambda_{max} - \Lambda_{min}}\right) \quad (4)$$

Where D is the Euclidean distance computed over the corresponding binary image and Λ is the gradient transform of the IHC image represented in the RGB space. Λ_{min} and Λ_{max} are the minimum and maximum values of the color gradient Λ needed for normalization.

Watershed algorithm is then applied on the inverse of the distance transformation D' using the following equation:

$$S = G_\sigma * \left(max\left(D'\right) - D'\right) \quad (5)$$

Here G_σ is a Gaussian smoothing operator used to reduce image noise with width σ=1.

However, as illustrated in Figure 5-a, the obtained separation results using the watershed method contain some over-segmented cases due to the intensity variations inside stained nuclei. This error is managed automatically using shape information to locate clustered nuclei and to enhance watershed segmentation results. In fact, touching and overlapping nuclei are first identified by the existence of high concavity points in nuclear boundaries shown in Figure 5-b. In our work, this task is done with a robust corner detector technique based on the global and local curvature features of the contour [6]. Then, the most significant separating edges within clustered nuclei are selected by searching the nearest end points of the inner edges to the concave vertices shown in Figure 5-c. We used here a local window (7×7) centered on the concave point to detect the minimal Euclidean distance between end points and concave vertices. After that, a weighted vertex graph G is constructed from the vertex set of selected inner edges E (white curves in Figure 5-c) and the set of end points V (red vertices in Figure 5-c). The nodes of the graph are then equal to $V \cup E$. Each node has an associated numerical value, called weight, which correspond in our work to the color gradient intensity Λ. Finally, to select the optimal separating curves of clustered nuclei, we have applied Dijkstra algorithm to compute the shortest path between the terminal vertices for each edge in the graph shown in Figure 5-d.

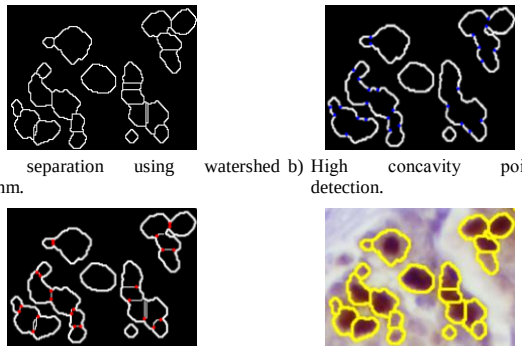

a) Nuclei separation using watershed algorithm. b) High concavity point's detection. c) Construction of the weighted graph through concave vertices. d) Optimal path selection using Dijkstra algorithm.

Figure 5. Clustered nuclei separation.

2.2.3. Benign Nuclei Removing

As illustrated in the flow chart of the automated nuclei segmentation method as shown in Figure 2, the second binary image obtained from the blue stain contains all nuclei (cancerous and non-cancerous nuclei). However, only the total number of positive and negative cancer nuclei is needed for evaluating the ER/PR status. For this reason, benign nuclei and stromal particles should be removed from the pre-segmented image. The key idea to detect B nuclei in this work is to design a criterion based on morphological features which are used by pathologists in their IHC analysis.

Benign nuclei are identified by the elliptic shape and the small size with respect to cancer nuclei. The elliptical shape can be modeled by the ratio E_r between major and minor axes of the ellipse and the size is evaluated by the number A of pixels in the nucleus region R. The proposed criterion for benign nuclei regions R_B is expressed as follows:

$$R_B(x,y) = \left\{ \begin{array}{c} R(x,y) / \left(E_r\left(R(x,y)\right) > E \; AND \; A\left(R(x,y)\right) < A_M\right) \\ OR \; A\left(R(x,y)\right) < A_m \end{array} \right\} \quad (6)$$

Experts expect that non-cancerous nuclei have an elliptic shape described by a ratio greater than a decision threshold E and an area lower than A_M. Benign nuclei may occur also with any form but their size is limited by another area bound A_m. We note that the decision thresholds are selected automatically by shape and size analysis. In our procedure, the ratio E is fixed at 1.55 and the lower bound and upper bound of the B nuclei area are determined by the average area of all detected nuclei $\overline{A}$, where $A_M = \overline{A}/1.5$ and $A_m = \overline{A}/3$ shown in Figure 4-f. The different steps of

the proposed nuclei segmentation approach are as follows:

- *Step 1*. Given the staining components (blue and brown) by color deconvolution method, apply to each intensity image adaptive thresholding using median filter with a neighborhood size equal to 22, 44 or 140 according to the image resolution $\times 20$, $\times 40$ or $\times 80$, respectively.
- *Step 2*. Construct the binary image of cell nuclei by applying dilatation and opening and holes filling. The two first morphological operations are performed using respectively a flat diamond-shaped structuring element with size R and $2R+1$, where R is chosen according to the size of the nuclei and the resolution of the image (R=2, 3 and 4) used respectively for a magnifying factor of $\times 20$, $\times 40$ and $\times 80$.
- *Step 3*. Apply the watershed algorithm on the inverse of the hybrid distance transform using (24) and (25).
- *Step 4*. Detect the concave vertices on the nuclei contours using the corner detection technique (see [6, 11] for more details).
- *Step 5*. Extract inner edges and find end points for each one of them.
- *Step 6*: Select the separating edge candidates (E) by searching the end points nearest to concave vertices (V).
- *Step 7*. For each edge candidate in the set E and each node of E, associate a weight value equal to the color gradient intensity.
- *Step 8*. Construct the weighted vertex graph G.
- *Step 9*. Find the shortest path between all detected end points in the graph using Dijkstra algorithm.
- *Step 10*. Add paths to nuclei contours to obtain final segmentation results.
- *Step 11*. Remove benign nuclei and stromal cells from the pre-segmented image of the blue component using (6).
- *Step 12*. Compute the number of separated nuclei for each segmented image.
- *Step 13*. Evaluate the percentage of positive cancer nuclei which is the fraction of number of brown stained nuclei per number of all detected cancer nuclei.

3. Results and Discussion

To demonstrate the effectiveness of the proposed nuclear segmentation method, nuclei quantification and cancer scoring results in our image database are provided in this section and compared to manual evaluation given by two experienced pathologists. The studied image database is composed of 84 breast cancer tissue images (1600×1200 pixels) taken with a light microscope OLYMPUS BX51 and CCD digital camera OLYMPUS DP21, using a magnifying factor of $\times 20$, $\times 40$ and $\times 80$. For each IHC image, the ER/PR positive status is determined by experts based on visual inspection of the staining intensity and a direct count of the proportion of positive nuclear staining in the malignant tissue.

The manual assessments and IHC analysis are then combined in a panel consensus which is considered as a gold standard for the evaluation of the proposed method. In this way, our image database is divided into three datasets according to the expert's positivity score (1+, 2+ or 3+) (see Table 1 for more details).

In Figure 6, we show experimental results of the proposed nuclear segmentation approach compared to two recent state of the art methods. Figures 6-b and c represent the splitting results of all detected nuclei using a marker-controlled watershed based on adaptive H-minima algorithm for markers selection [3] and an improved watershed method with multi-marker merging procedure [13], respectively. As illustrated in Figure 6, both H-minima marker-guided watershed and multimarker-controlled watershed approaches provide good segmentation results in different overlapping and complex nuclear configurations. But we can clearly notice erroneous segmentations in some few cases, such as under-segmented nuclei (red arrows) and over-segmented nuclei (white arrows). These problems are significantly solved using the proposed separation method and more efficient results can be seen Figure 6-d.

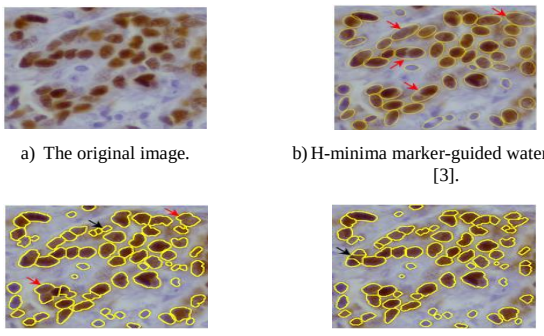

a) The original image. b) H-minima marker-guided watershed [3]. c) Multimarker-controlled watershed method [13]. d) The proposed method.

Figure 6. Splitting results of all detected cell nuclei.

Table 2. Comparative separation results of touching nuclei on the complete image database using H-minima marker-controlled watershed algorithm [3], multimarker-controlled watershed method [13] and the proposed separation method: watershed and weighted concave vertex graph.

	H-minima Marker-Controlled Watershed	**Multimarker-Controlled Watershed**	**Watershed and Weighted Concave Vertex Graph**
Correctly segmented nuclei (%)	68.72 ± 2.29	90.23 ± 1.57	96.85 ± 0.95
Over-segmented nuclei (%)	30.55 ± 1.92	0.23 ± 0.13	0.92 ± 0.20
Under-segmented nuclei (%)	0.73 ± 0.97	9.54 ± 0.92	2.23 ± 0.62
Total computation time (s)	39.11 ± 0.12	99.45 ± 1.57	47.62 ± 0.54

The quantitative results presented in Table 2 show that the proposed method is more efficient in touching nuclei separation than the other studied approaches. In fact, the segmentation results are recognized into three groups: Correctly segmented, over-segmented, and under-segmented touching nuclei. The proposed method performs improvements by 28.13±1.34%, and 6.62±0.62% with respect to H-minima marker-guided watershed and multimarker-controlled watershed algorithms in terms of separation accuracy, respectively. Moreover, the computation time results show that the proposed method is faster than the multimarker-controlled watershed [13] which is considerably accurate than the H-minima marker-controlled watershed [3].

Table 3. Results of the computer-assisted ER/PR evaluation system versus expert's assessment on the complete image database.

	Computer-assisted ER/PR evaluation			Expert's assessment		
	Dataset (1+)	Dataset (2+)	Dataset (3+)	Dataset (1+)	Dataset (2+)	Dataset (3+)
True positive nuclei	1402	2742	1520	1436	2756	1524
False positive nuclei	43	51	12	0	0	0
True negative nuclei	956	1597	446	987	1632	459
False negative nuclei	55	62	18	0	0	0
Sensitivity (%)	96.2	97.7	98.8	100	100	100
Specificity (%)	95.7	96.9	97.3	100	100	100
Accuracy (%)	96	97.4	98.5	100	100	100
Total number of images	31	42	11	32	42	10
False classified images	0	1	1	0	0	0
Scoring accuracy (%)	97.6			100		

In Table 3, we report the statistical analysis in terms of sensitivity, specificity and accuracy of positive and negative cell nuclei. We provide also the cancer scoring results on the complete image database. The obtained quantification and scoring results of the proposed scheme are compared in Table 3 with manual evaluation provided by pathologists. From these experiments, we demonstrate the high precision of the proposed segmentation method on a large database of real-life breast tissue images. Compared to the nuclei quantification provided by experts, the proposed method is able to detect cancer nuclei with an average accuracy of 97.3% in the whole image database. Furthermore, in assigning the cancer score of each case, the automated image analysis method gives 97.6% in overall accuracy, ranking correctly 82/84 cases.

The efficiency of the method can be clearly notified in Figure 7, by comparing the segmentation results of our method and the ground truth from the pathologist panel. A high agreement can be clearly seen, in Figure 7, between detected cancer nuclei using the proposed method and manually marked nuclei, especially for positive staining. However, we note some false benign nuclei detected by the automated approach that can lead to a weak error (less than 4%) on cancer scoring in the whole image. This problem is due particularly to the under-segmented nuclei produced by the nuclei separation procedure in some case of complex cell nuclei configurations. With these results, we conclude that the proposed image analysis method can reliably be used to assist pathologists in their diagnosis, by providing a second opinion for ambiguous cases that require further attention.

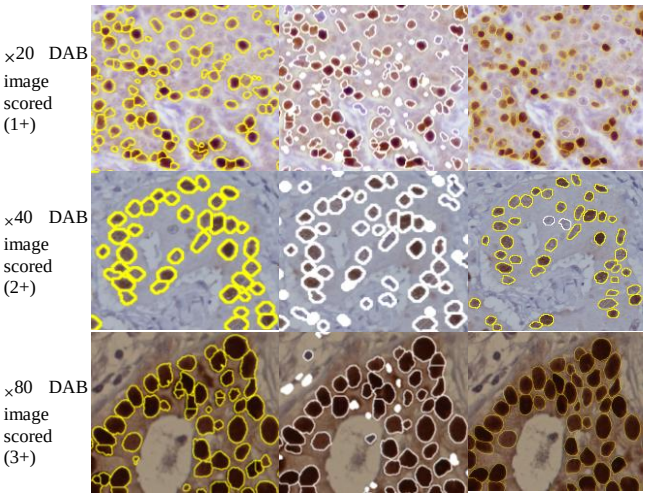

a) Automated segmentation of positive cancer nuclei. b) Automated segmentation of all cancer nuclei. c) Manual segmentation of all cancer nuclei provided by experts.

Figure 7. Segmentation results of positive nuclear staining. Where yellow contours delimit P cancer nuclei and the white ones delineate the N cancer nuclei.

4. Conclusions

In this paper, we proposed an automated image segmentation method for evaluating the ER/PR status in breast cancer specimens. The proposed method combines a color deconvolution method and an improved morphological procedure based on the watershed algorithm for cell nuclei segmentation. The method is tested on a real-life image database containing the three degrees of malignancy (1+, 2+ and 3+). Besides, the obtained results are compared with the truths given by pathologists, achieving more than 97% in overall accuracy of nuclei quantification and an agreement of 97.6% in cancer scoring of the studied database. In conclusion, the proposed segmentation method for automatic assessment of ER/PR status in IHC stained breast sections can reliably be used as an additional tool to assist pathologists in the cancer diagnosis process.

References

[1] Brey E., Lalani Z., Johnston C., Wong M., McIntire L., Duke P., and Patrick J., "Automated Selection of DAB-Labeled Tissue for Immunohistochemical Quantification," *Journal of Histochemistry and Cytochemistry*, vol. 51, no. 5, pp. 575-584, 2003.

[2] Cataldo D., Ficarra E., Acquaviva A., and Macii E., "Automated Segmentation of Tissue Images for Computerized IHC Analysis," *Computer Methods and Programs in Biomedicine*, vol. 100, no. 1, pp. 1-15, 2010.

[3] Cheng J. and Rajapakse J., "Segmentation of Clustered nuclei with Shape Markers and Marking Function," *IEEE Transactions on Biomedical Engineering*, vol. 56, no. 3, pp. 741-748, 2009.

[4] Gurcan M., Boucheron L., Can A., Madabhushi A., Rajpoot N., and Yener B., "Histopathological Image Analysis: a Review," *IEEE Reviews in Biomedical Engineering*, vol. 2, pp. 147-171, 2009.

[5] He L., Long L., Antani S., and Thoma G., "Histology Image Analysis for Carcinoma Detection and Grading," *Computer Methods Programs Biomedicine*, vol. 107, no. 3, pp. 538-556, 2012.

[6] He X. and Yung N., "Corner detector Based on Global and Local Curvature Properties," *Optical Engineering*, vol. 47, no. 5, pp. 1-12, 2008.

[7] Leake R., Barnes D., Pinder S., Ellis I., Anderson L., Anderson T., Adamson R., Rhodes T., Miller K., and Walker R., "Immunohistochemical Detection of Steroid Receptors in Breast Cancer: a Working Protocol," *Journal of Clinical Pathology*, vol. 53, no. 8, pp. 634-635, 2000.

[8] Lin G., Adiga U., Olson K., Guzowski J., Barnes C., and Roysam B., "A Hybrid 3D Watershed Algorithm Incorporating Gradient Cues and Object Models for Automatic Segmentation of Nuclei in Confocal Image Stacks," *Wiley InterScience*, vol. 56A, no. 1, pp. 23-36, 2003.

[9] Loukas C. and Linney A., "A Survey on Histological Image Analysis-Based Assessment of Three Major Biological Factors Influencing Radiotherapy: Proliferation, Hypoxia and Vasculature," *Computer Methods and Programs in Biomedicine*, vol. 74, no. 3, pp. 183-199, 2004.

[10] Madzin H., Zainuddin R., and Mohamed N., "Analysis of Visual Features in Local Descriptor for Multi-Modality Medical Image," *The International Arab Journal of Information Technology*, vol. 11, no. 5, pp. 468-475, 2014.

[11] Mouelhi A., Sayadi M., Fnaiech F., Mrad K., and Romdhane K., "Automatic Image Segmentation of Nuclear Stained Breast Tissue Sections Using Color Active Contour Model and an Improved Watershed Method," *Biomedical Signal Processing and Control*, vol. 8, no. 5, pp. 421-436, 2013.

[12] Ruifrok A. and Johnston D., "Quantification of Histochemical Staining by Color Deconvolution," *Analytical and Quantitative Cytology and Histology*, vol. 23, no. 4, pp. 291-299, 2001.

[13] Veta M., Diest P., Kornegoor R., Huisman A., Viergever M., and Pluim J., "Automatic Nuclei Segmentation in H and E Stained Breast Cancer Histopathology Images," *PLoS One*, vol. 8, no. 7, 2013.

[14] Vincent L. and Soille P., "Watersheds In Digital Spaces: An Efficient Algorithm Based on Immersion Simulations," *IEEE Transactions on Pattern Analysis and Machine Intelligence.* vol. 13, no, 6, pp. 583-598, 1991.

Aymen Mouelhi was born in Tunis in 1981 (Tunisia). He received the B.Sc. degree in electrical engineering from the Higher School of Sciences and Techniques of Tunis (ESSTT), the M.Sc. degree in automatic control and the Ph.D. degree in signal and image processing from the same school, respectively in 2003, 2006 and 2014. He is a member of research group in Laboratory of Signal Image and Energy Mastery (SIME) of the University of Tunis. His research interests include image processing, classification and intelligent data processing for cancer diagnosis.

Mounir Sayadi born in 1970 in Tunis (Tunisia), he received the B.Sc. degree in Electrical Engineering from the High School of Sciences and Techniques of Tunis, the DEA degree in Automatic and Signal Processing from same school and the Ph.D. degree in signal processing from the National School of engineers of Tunis, respectively in 1992, 1994 and 1998. He is currently Professor at the National Superior School of Engineers of Tunis (ENSIT) and member of the Laboratory of Signal Image and Energy Mastery SIME. Dr. Sayadi has published over 25 research journal papers and 95 scholarly communications in many international conferences. His research interests are focused on adaptive signal processing and filtering, medical image and texture classification and segmentation.

Farhat Fnaiech born in 1955 in la Chebba (Tunisia), he received the B.Sc. degree in Mechanical Engineering in 1978 from the High school of sciences and techniques of Tunis and the master degree in 1980, the Ph.D. degree from the same school in Electrical Engineering in 1983, and the Doctorate Es Science in Physics from the Faculty of Sciences of Tunis in 1999. He is currently Professor at the National Superior School of Engineers of Tunis (ENSIT). Prof. Fnaiech is Senior Member IEEE and has published over 150 research papers in many journals and international conferences. He was the general chairman and member of the international Board committee of many International Conferences.
His is Associate Editor of IEEE Transactions Industrial Electronics. He is serving as IEEE Chapter committee coordination sub-committee delegate of Africa Region 8. His main interest research areas are nonlinear adaptive signal processing, nonlinear control of power electronic devises, digital signal and image processing and intelligent techniques and control.

Karima Mrad was born in Tunis in 1968 (Tunisia). She received the Ph.D. degree in pathology and anatomical sciences from University of Paris V (France) in 2003. She is actually a professor in the University of Medicine of Tunis and a head service of anatomy and pathology department at Salah Azaiez Cancer Institute, Tunis. Her main interest research areas are histopathology, immunohistochemistry and cancer diagnosis.